

Electrochemical and Mechanical Behavior in Polycrystalline Co-Ni-Ga Shape Memory Alloys

M. Sanchez-Carrillo¹, J. P. Flores de los Rios¹, E. Huape-Padilla¹, R.G. Bautista Margulis^{3,*},
H. Flores-Zuñiga², M.I. Ferrer-Sanchez³, G. López-Ocaña³, J.G. Chacón-Nava¹,
A. Martínez-Villafañe¹

¹ Departamento de Metalurgia e Integridad Estructural, Centro de Investigación en Materiales Avanzados, S.C., Miguel de Cervantes 120, Complejo Ind. Chihuahua, C.P. 31109, Chihuahua. Chih. México.

² División de Materiales Avanzados, Instituto Potosino de Investigación Científica y Tecnológica A. C., Camino a la Presa de San José # 2055. Lomas 4a. Secc. 78216 San Luis Potosí, S.L.P. México.

³ División Académica de Ciencias Biológicas, Universidad Juárez Autónoma de Tabasco, C.P. 86040, Villahermosa, Tabasco, México.

*E-mail: margulisrg@hotmail.com

Received: 9 September 2014 / Accepted: 6 October 2014 / Published: 28 October 2014

Electrochemical behavior and microstructure was studied in polycrystalline $\text{Co}_{38.3}\text{Ni}_{32.1}\text{Ga}_{29.6}$ alloy using the electrochemical technique of polarization curves in a medium of 3.5 wt % NaCl and 0.5M H_2SO_4 . The importance of these alloys is due to their functional behavior, as shape memory alloys with ferromagnetic properties. The alloy was fabricated by induction furnace and the characterizations were performed using differential scanning calorimetry (DSC), nanoindenter tests and X-ray diffraction (XRD) The analysis of the kinetics of corrosion was conducted using cyclic sweep voltammetry curves with potentiostat/galvanostat. The corrosion morphologies were also analyzed by scanning electron microscopy (SEM). The kinetics of corrosion was found to be highest in the acid media and the alloy with thermal treatment in 3.5 wt% NaCl (A-TT-NaCl) shows a i_{corr} lower than the alloy without thermal treatment (A-NaCl) in the same solution. On polarization curves, the current alloys exhibited a general dissolution in the anodic branch until certain potential was reached where a spontaneous passive zone occurred in 3.5 wt% NaCl media, similar behavior was found in acid media where, under high potentials occurs a repassivation zone at 427mV and elements such as Co and Ni were present in a higher percentage for all the corrosion deposits.

Keywords: shape memory alloys, polarization curves, polycrystalline, nanoindentation, calorimetry, corrosion deposits.

1. INTRODUCTION

Ferromagnetic shape memory alloys have received much attention because they exhibit both magnetic field induced strain and magnetic shape memory effect. The alloys of the system Ni-Mn-Ga close to the stoichiometric composition 2-1-1 are type Heusler alloys. These alloys exhibit a martensitic transformation which is related to the memory effect. Since the discovery of large strains (up to 10%) induced by the magnetic field in the ferromagnetic alloys near stoichiometric composition Ni₂-Mn-Ga, has been of growing interest in the research and development of these alloys due to the wide range of expected applications [1, 2]. Potential applications of this type of alloy are actuators, MEM's [3] strain sensors [4] or vibration dampers [5]. Studies on the shape memory alloys of Ni-Mn-Ga show a response to external stimuli at temperatures near to the transition. Stress and the magnetic field is effective in inducing a transition, giving rise to large deformation and changes in magnetization [6]. These changes provide additional properties to this class of materials, such as the elastocaloric effect [7] and the magnetocaloric [8] which are of interest for applications in solid state cooling near to the room temperature [9]. However, the fragility of this material is a limiting factor for practical applications.

Studies on several candidates for ferromagnetic shape memory alloys have been carried out: Fe-Pd [10], Fe-Pt [11], Ni-Mn-Al [12], and Co-Ni-Al [13, 14] in order to find out new alternative materials with lower brittleness. Recently, Ni-Fe-Al [15] and Co-Ni-Ga [16] have been considered as good ferromagnetic shape memory alloys candidates, mainly due to the presence of a γ phase (disordered fcc Al) that improves ductility in these kind of alloys [17, 18], but a high percentage of this phase can cause a decrease of magnetically induced strain. In contrast with Ni-Mn-Ga alloys, these new Co- and Ni-based alloys usually present dual-phase structures. This behavior was also found in Co-Ni-Al [17], Ni-Al-Fe [19] and Ni-Fe-Ga [20].

Since the applications of ferromagnetic shape memory alloys experience a large change of shape, corrosion protection with additional coatings would be nearly impossible. Therefore, these alloys must exhibit high resistance "intrinsic" to corrosion attack and a high surface self-healing ability. However, up to date corrosion studies of ferromagnetic shape memory alloys Co-Ni-Ga are scarce and mostly for Ni-Mn-Ga systems and have led in part to controversial conclusions [21-23]. The aim of this paper is to determine the corrosion behavior in two different media of Co-Ni-Ga polycrystalline ferromagnetic shape memory alloys in aqueous solution of NaCl 3.5 wt % and 0.5M H₂SO₄ by cyclic polarization and the microstructural characterization.

2. EXPERIMENTAL PROCEDURE

Polycrystalline ingots of Co-Ni-Ga were prepared by induction melting furnace under argon atmosphere. The alloys were re-melted two times to improve homogeneity. The materials used for casting were pure elements Co (99.9%), Ni (99.9%), and Ga (99.99%), then ingot slices were extracted and encapsulated in a quartz tube for a heat treatment in vacuum atmosphere. Heat treatment was applied to improve homogeneity and structural ordering at temperature of 1100°C for 24 h and 900 °C

for 24 h and subsequently quenching in water. Material slices were cut from the ingots by a wire-cutting machine with diamond paste to get a defined cross sectional area and thereby perform electrochemical tests. Likewise these slices were used to other types of analysis.

Each alloy was characterized by Differential Scanning Calorimetry (DSC) using a DSC calorimeter Q200 TA instruments, using a heating and cooling speed of 10 °C/min at interval from 0°C to 550°C and samples about 20 mg in average. Calorimetric data were recorded during heating and cooling runs of Co_{38.3}Ni_{32.1}Ga_{29.6} alloy, as shown in figure 1. The chemical composition of the alloy and its corrosion products were determined by means of X-ray Energy Dispersive (EDS) Spectroscopy in a JEOL JSM-5800LV microscope. The size of the area was 0.5mm X 0.5mm after annealing treatment. The phase structure was identified on bulk samples at room temperature by using an X-ray diffractometer Xpert MPD Phillips ($\theta - 2\theta$) with Cu K α radiation. Table 1 presents the composition and the transition temperatures of studied alloy.

Table 1. Composition and transition temperatures of the studied alloy.

Muestra	Co at. %	Ni at. %	Ga at. %	A _s °C	A _f °C	M _s °C	M _f °C
A-TT	38.3	32.1	29.6	450.9	490.3	316.9	275.8

(±0.25%)

For the corrosion tests the material used was electrical connected to a copper wire and spot welded, and then each specimen was encapsulated in epoxy resin for mechanically polished to 4000 grit and then rinsed with alcohol and dried. Electrochemical experiments were performed on a conventional three-electrode cell of platinum wire as auxiliary electrode, saturated calomel electrode (SCE) as a reference and the working electrode, which is the shape memory alloy using cyclic sweep voltammetry. The electrochemical cell was connected to a potentiostat/galvanostat AUTOLAB equipment AUT84861 model. The electrolyte used was a solution of 3.5 wt% NaCl and 0.5M H₂SO₄ solution prepared with analytical grade chemicals and distilled water and the temperature was held at 25 °C (±2°C). Before starting the polarization experiment, the specimen was immersed in the electrolyte half an hour, thus allowing stabilizing the corrosion potential in the system. The potentiostatic polarization measurements of full cycle were performed with a scan rate of 0.5 mV/s in a range of -1200mV to 900mV_{SCE}. The polarization resistance (Rp) was converted to a corrosion rate in mm/year ($vel_{mm/year}$) according to the following equations:

$$Vel_{mm/year} = \frac{0.00327 (i_{corr})EW}{\rho} \quad (1)$$

$$i_{corr} = \frac{B_a B_c}{2.303 R_p (B_a + B_c)} \quad (2)$$

Where i_{corr} is the corrosion current density ($\mu\text{A}/\text{cm}^2$), EW is the equivalent weight (chemical) of alloy calculated according to ASTM G102-89(2010), ρ is the density of the alloy (g/cm^3), Rp is the

polarization resistance ($\Omega \text{ cm}^2$), B_a and B_c (mV) are the slopes of anodic and cathodic Tafel plot. Nanoindentation test were performed on Indenter Agilent Technologies G-200. The head used was DCM with Berkovich indenter type. (20nm) in order to know the mechanical properties of the phase present on the alloy. The microstructure was examined by optical microscopy using a chemical etching solution consisting of 25% HNO_3 –ethanol.

3. RESULTS AND DISCUSSION

The martensitic and austenitic transformation temperatures and composition are observed in figure 1. The alloy shows a martensitic transition known as at high temperature around 300°C and the austenitic transition is 450°C and ends around 490°C .

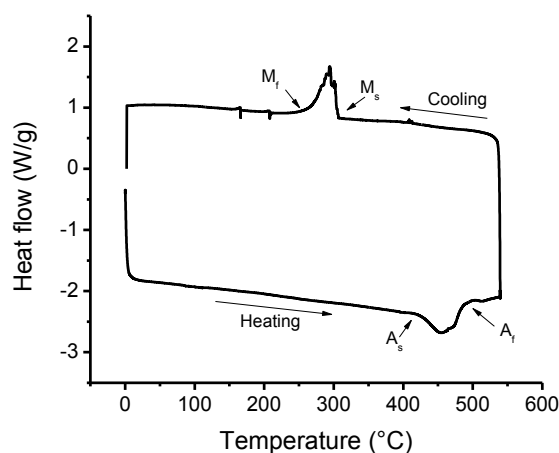


Figure 1. Calorimetric curves during heating and cooling from the alloy.

Optical microscopy (OM) is shown in figure 2, where γ -phase precipitates and the martensitic phase were present. The sample consists of martensitic and γ phase with the hardness values of 7 ± 0.4 GPa and 6.1 ± 0.2 GPa, respectively, indicating the soft nature of the γ -phase.

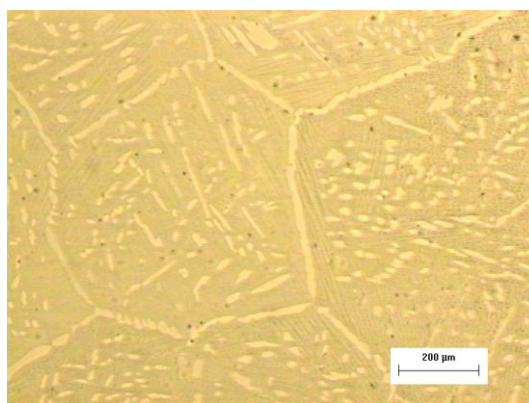


Figure 2. Microstructure of the studied alloy A-TT.

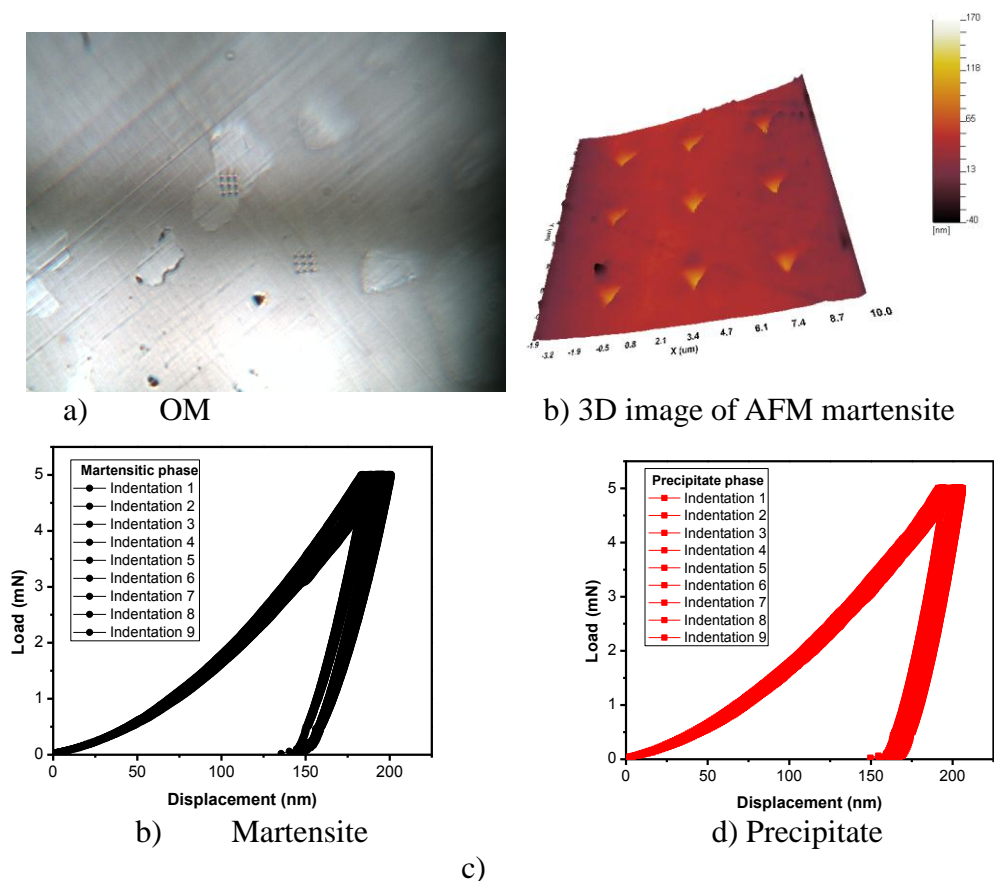


Figure 3. a) OM, b) image of AFM and c) and d) load-displacement (P-h) curves of Co-Ni-Ga phases.

The results of load-displacement curves from figure 3 are shown in table 2.

Table 2. Nanoindentation results from displacement-load graphs.

Phase analyzed	Martensitic phase	Precipitate phase
H (GPa)	7 ±0.3	6.1 ±0.2
E (GPa)	186.8 ±10.5	209.5 ±9.1

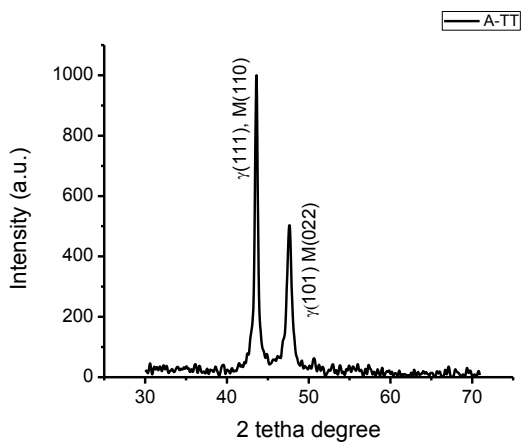


Figure 4. X-ray diffraction pattern for alloy A-TT at room temperature.

Nanoindentation test were performed on the existing phases, it allowed the determination of elastic modulus (E) and the hardness (H) of martensitic and precipitate phases. According to Figure 3, It was found that the material has an elasto-plastic nature obtained from elastic recovery ratio [24].

Figure 4 shows a typical X-ray diffraction pattern of the alloy at room temperature. The diffraction pattern shows a two-phase structure where the precipitate phases do not martensitically transform but this γ -phase improves the ductility of the alloy.

3.1 Cyclic polarization curves

Electrochemical characterization of shape memory alloys of $\text{Co}_{38.3}\text{Ni}_{32.1}\text{Ga}_{29.6}$ was tested in an aqueous solution of 3.5 wt% NaCl and 0.5M H_2SO_4 at room temperature. Figure 5 shows the cyclic polarization curves with different media and for alloy with thermal treatment and without.

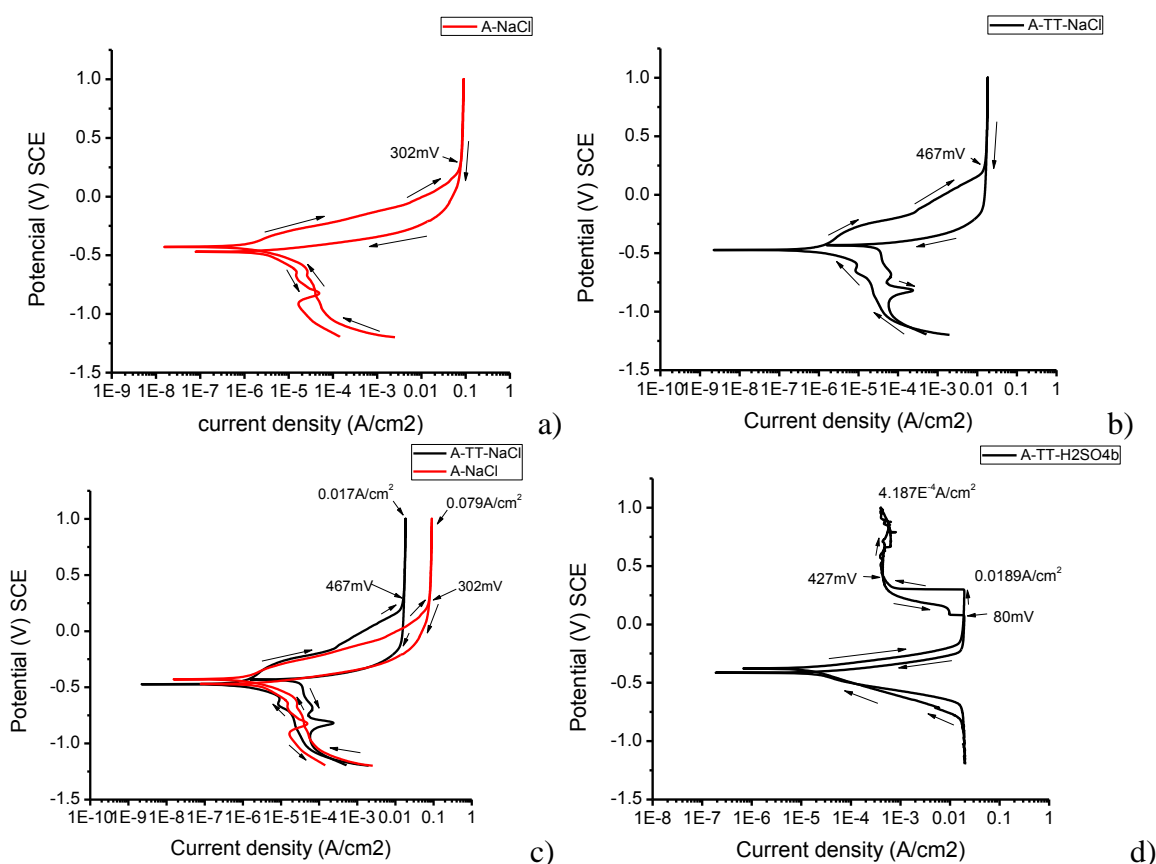


Figure 5. Polarization curves in Co-Ni-Ga, a) without TT, b) with TT, c) comparative a and b in an electrolyte of 3.5 wt% of NaCl and d) with TT in electrolyte of 0.5M H_2SO_4 with a sweep rate of 0.5 mV/s for all test.

From the plots in figure 5, current densities values (i_{corr}) and corrosion potential E_{corr} were obtained and showing that potentials are around -400mV in 3.5% wt NaCl and the acid media are -377mV. The i_{corr} decreases with thermal treatment in electrolyte of 3.5 wt % NaCl and its increase some orders of magnitude in acid media. The repetitions (at least two) of the tests were consistent

corroborating the reproducibility behavior presented by the alloys. Corrosion parameters generated from the analysis of the potentiodynamic polarization curves are shown in Table 3; The Tafel slopes were obtained by linear fitting of the potentiodynamic polarization data within ± 50 to ± 100 mV of the E_{corr} , note that the E_{corr} of A alloy in 3.5 wt % NaCl is lower than A-TT indicating that A alloy is more active in this media under used conditions. Alloy A-TT presents the higher i_{corr} a light different behavior because after spontaneous passivation presents a tendency of second passivity at potential around 427 mV and a decreasing the i_{corr} some orders of magnitude, after that the return path shows a break down potential around 80 mV in the first passive zone. Figure 6 illustrates clearly the tendency of the i_{corr} in each of the media tested, showing that the most aggressive media was the acid that has the highest i_{corr} and on the other hand the lower i_{corr} was for the alloy with thermal treatment in a neutral media. This implies that the TT enhances i_{corr} in the same media according to the results in electrolyte of 3.5 wt% NaCl.

Table 3. Electrochemical parameters of the polarization curves in electrolyte with 3.5 wt% NaCl and 0.5M H₂SO₄.

A and A-TT alloys			
media	3.5% wt NaCl no TT	3.5% wt NaCl	0.5M H ₂ SO ₄
i_{corr} (nA/cm ²)	480.59	347.77	4042
E_{corr} (mV) _{SCE}	-433	-475	-377
Vel. (mm/year)	0.0044	0.00324	0.0377

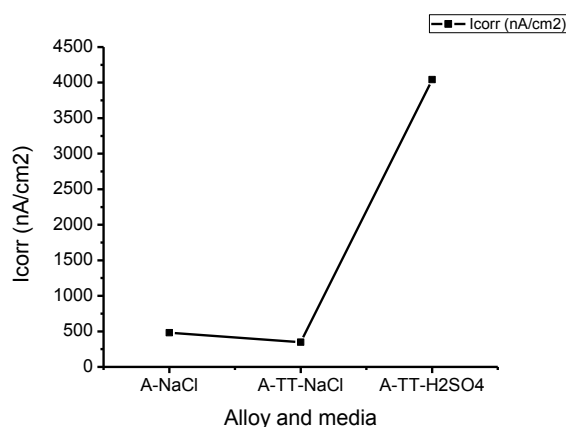


Figure 6. Behavior of i_{corr} and its relationship with media and studied alloys.

According to the graphs in Figure 5, the general behavior is active-passive, i.e. the anodic branch presents a general dissolution of the alloy, and thus increasing the current density up to a value where then presents a spontaneous passive behavior [25]. Gebert et al [26] conducted electrochemical experiments in shape memory alloys of polycrystalline Ni-Mn-Ga where the pH values neutral and alkaline showed polarization curves with a tendency of spontaneous passivation of sample surface and under these conditions did not see a noticeable difference in behavior either martensite or austenite. For the current results presented in Figure 5, no transpassivity effect was observed even when the

potential sweep values were found to be about 1 volt. This behavior may be due to the type of alloy, contrary to the results obtained by Gebert et al. [26] where it has a slight transpassivity response in potential of about 0.5V and neutral pH.

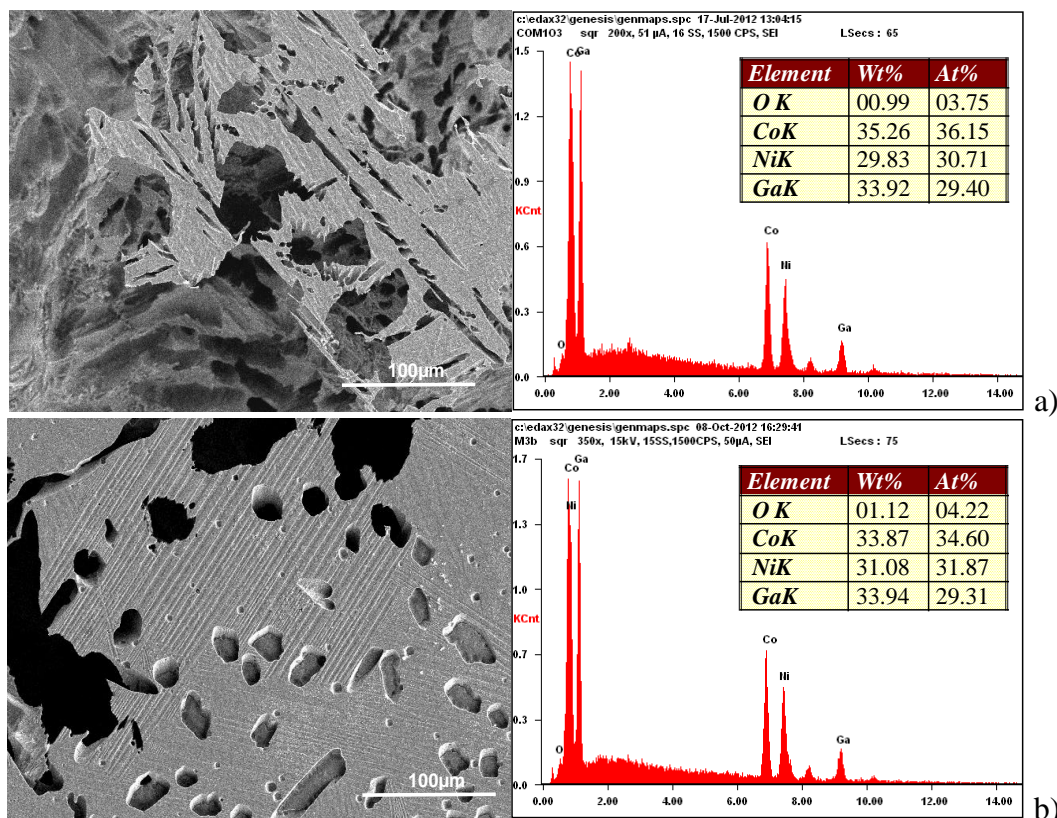


Figure 6. Images of scanning electron microscopy after electrochemical test which showed the environmental deterioration of alloy a) without thermal treatment and b) with thermal treatment generated by electrolyte 3.5 wt% NaCl, at 350x, and its corresponding EDS analysis.

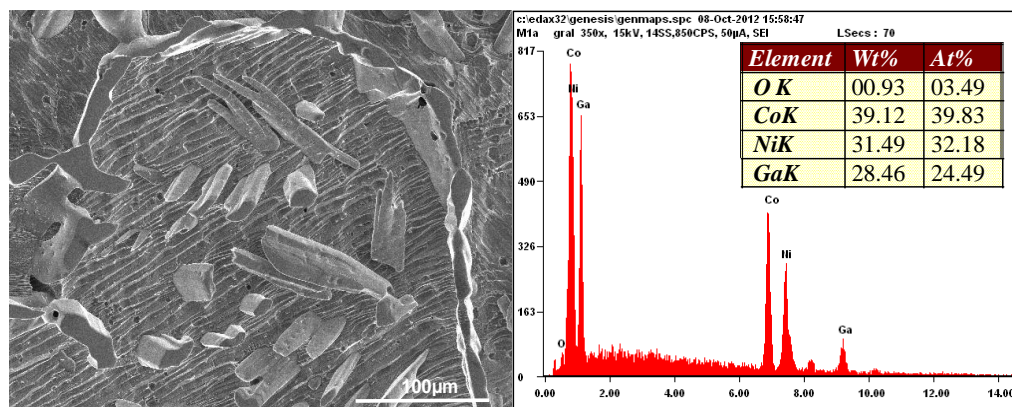


Figure 7. Images of scanning electron microscopy after electrochemical test which showed the environmental deterioration of sample tested with thermal treatment generated by electrolyte 0.5M H₂SO₄, at 350x and its corresponding EDS analysis.

Likewise it shows that the reverse sweep follows along the same path which could be an indication that the material has no tendency to localized corrosion [27], except figure 5d where we found that after spontaneous passivation presents a tendency of another passivity at potential around 427mV and a decreasing the i_{corr} some orders of magnitude, after that the return path shows a break down potential around 80mV in the first passive zone. These graphs (Figure 5a and 5b) also showed a slope of low breakdown potential that are associated with an increased propagation of pitting, but when they had long hysteresis could be an indication of material being susceptible to pitting [23].

From the various samples tested (see Figure 6 and 7), it is clearly noted that the attack was very aggressive for the alloy showing a general dissolution without the presence of a localized attack according to polarization curves; while in figure 6a particularly, an aggressive attack was observed. Figure 6b presents morphology with some martensitic phase present and most of superficial area was protected in comparison to figure 6a. From the results showed in Figure 7, the attack by acid media shows a selected dissolution leaving the precipitates superficially.

During the study of the morphology, the material was analyzed by X-ray energy dispersive spectroscopy (EDS) to identify the elements present on the deteriorated surface and some selected areas.

Figure 6a and 6b and figure 7 have a general EDS where, according to the values in the table, there is a substantial amount of Co and Ni such as Ga and O by weight. This implies that the presence of oxygen plays an important role in the protection of this kind of alloys.

4. CONCLUSIONS

From the current results obtained in this research work, it can be concluded the following:

- a) With the alloys used in this study i_{corr} decreases with thermal treatment in electrolyte of 3.5 wt % NaCl.
- b) The most aggressive media for this type of alloy was 0.5M H₂SO₄.
- c) According to the results of polarization curves, the current alloy exhibited a general dissolution in the anodic branch until certain potential is reached where a spontaneous passive zone occur for electrolyte 3.5 wt% NaCl.
- d) Polarization curves for 0.5M H₂SO₄ showed a similar behavior for the 3.5 wt% NaCl until potential around 427mV shows decreasing the i_{corr} some orders of magnitude to another passive zone, after that the return path shows a break down potential around 80mV.
- e) Elements such as Co and Ni were present in a higher percentage plus oxygen determined by EDS.
- f) The morphology showed after electrochemical test was very aggressive according to micrographs.

ACKNOWLEDGEMENTS

The authors acknowledge financial support received from CONACYT, Mexico, under Project CB-2010-01-157541. The technical assistance by Enrique Torres, Daniel Lardizabal, Adan Borunda, Karla

Campos, Victor Orozco, Roberto Talamantes-Soto, Jair Lugo Cuevas and Gregorio Vazquez-Olvera is gratefully acknowledged.

References

1. K. Ullakko, J. Huang, C. Kantner, R. O'handley, V. Kokorin, *Applied Physics Letters*, 69 (1996) 1966.
2. P. Mullner, V. Chernenko, G. Kostorz, *Journal of applied physics*, 95 (2004) 1531-1536.
3. M. Kohl, D. Brugger, M. Ohtsuka, T. Takagi, *Sensors and Actuators A: Physical*, 114 (2004) 445-450.
4. N. Sarawate, M. Dapino, *Applied Physics Letters*, 88 (2006) 121923-121923-121923.
5. J. Feuchtwanger, K. Griffin, J. Huang, D. Bono, R.C. O'Handley, S.M. Allen, *Journal of magnetism and magnetic materials*, 272 (2004) 2038-2039.
6. O. Söderberg, A. Sozinov, Y. Ge, S.-P. Hannula, V. Lindroos, *Handbook of magnetic materials*, 16 (2006) 1-39.
7. E. Bonnot, R. Romero, L. Mañosa, E. Vives, A. Planes, *Physical review letters*, 100 (2008) 125901.
8. A. Planes, L. Manosa, M. Acet, *Journal of Physics: Condensed Matter*, 21 (2009) 233201.
9. K.A. Gschneidner Jr, V. Pecharsky, A. Tsokol, *Reports on Progress in Physics*, 68 (2005) 1479.
10. R.D. James, M. Wuttig, *Philosophical Magazine A*, 77 (1998) 1273-1299.
11. T. Kakeshita, T. Takeuchi, T. Fukuda, T. Saburi, R. Oshima, S. Muto, K. Kishio, *JIM, Materials Transactions*, 41 (2000) 882-887.
12. F. Gejima, Y. Sutou, R. Kainuma, K. Ishida, *Metallurgical and Materials Transactions A*, 30 (1999) 2721-2723.
13. K. Oikawa, L. Wulff, T. Iijima, F. Gejima, T. Ohmori, A. Fujita, K. Fukamichi, R. Kainuma, K. Ishida, *Applied Physics Letters*, 79 (2001) 3290-3292.
14. H. Morito, A. Fujita, K. Fukamichi, R. Kainuma, K. Ishida, K. Oikawa, *Applied Physics Letters*, 81 (2002) 1657-1659.
15. S. Kaul, B.A. D'Santhoshini, A. Abhyankar, L.F. Barquin, P. Henry, *Applied Physics Letters*, 89 (2006) 093119.
16. K. Oikawa, T. Ota, F. Gejima, T. Ohmori, R. Kainuma, K. Ishida, *Materials Transactions-JIM*, 42 (2001) 2472-2475.
17. R. Kainuma, M. Ise, C.-C. Jia, H. Ohtani, K. Ishida, *Intermetallics*, 4 (1996) S151-S158.
18. A. Tejada-Cruz, F. Alvarado-Hernández, D. Soto-Parra, R. Ochoa-Gamboa, P. Castillo-Villa, H. Flores-Zúñiga, S. Haro-Rodríguez, A. Santos-Beltrán, D. Ríos-Jara, *Journal of Alloys and Compounds*, 499 (2010) 183-186.
19. R. Kainuma, S. Imano, H. Ohtani, K. Ishida, *Intermetallics*, 4 (1996) 37-45.
20. T. Omori, N. Kamiya, Y. Sutou, K. Oikawa, R. Kainuma, K. Ishida, *Materials Science and Engineering: A*, 378 (2004) 403-408.
21. X. Liu, O. Söderberg, Y. Ge, N. Lanska, K. Ullakko, V. Lindroos, in: *Journal de Physique IV* (Proceedings), EDP sciences, 2003, pp. 935-938.
22. A. Sozinov, O. Söderberg, V. Lindroos, Y. Ge, X.W. Liu, in: *Materials Science Forum, Trans Tech Publ*, 2002, pp. 565-568.
23. L. Stepan, D. Levi, E. Gans, K. Mohanchandra, M. Ujihara, G. Carman, *Journal of Biomedical Materials Research Part A*, 82 (2007) 768-776.
24. A. Annadurai, *International Journal of Engineering and Technology*, (2012).
25. B. Guo, Y. Tong, F. Chen, Y. Zheng, L. Li, C. Chung, *Materials and Corrosion*, 63 (2012) 259-263.

26. A. Gebert, S. Roth, S. Oswald, L. Schultz, *Corrosion Science*, 51 (2009) 1163-1171.
27. J.O. Alvarado Cortés, (2006).

© 2014 The Authors. Published by ESG (www.electrochemsci.org). This article is an open access article distributed under the terms and conditions of the Creative Commons Attribution license (<http://creativecommons.org/licenses/by/4.0/>).